JAPAN RESEARCH ON COMPATIBILITY IMPROVEMENT AND TEST PROCEDURES

Koji Mizuno
Nagoya University
Kunio Yamazaki
Yuji Arai
Japan Automobile Research Institute
Masao Notsu
Ministry of Land, Infrastructure and Transport (MLIT)
Japan
Paper Number 05-0185

ABSTRACT

This paper summarizes the compatibility research project conducted by JMLIT. Test procedures to assess vehicle compatibility were investigated based on a series of crash tests. In the IHRA (International Harmonized Research Activities) Compatibility Working Group, the full-width tests have been agreed upon for structural interaction evaluation of the Phase 1 approach. Thus, the JMLIT compatibility research project mainly focused on this test procedure.

Full-width rigid and deformable barrier tests were compared with respect to force distributions, vehicle deformation and dummy responses. In full-width deformable barrier tests, shear deformations are excited, and forces from structures can be clearly shown in barrier force distributions. The average height of force (AHOF) determined in full-width rigid and deformable barrier tests was similar. Basically, the full-width deformable barrier tests can be used as high acceleration tests. The dummy injury criteria were also similar between full-width rigid and deformable barrier tests, although for small cars the injury criteria can be inferior for full-width deformable barrier test due to sensor delay.

In order to investigate SEAS detection in the barrier force distributions, full-width tests were conducted for SUVs (sport utility vehicles) with and without SEAS. The reaction force of the SEAS could be detected in the full-width deformable barrier test. The VNT (vertical component of negative deviation from target row load) will be a useful criterion to evaluate the SEAS reaction force.

Car-to-car crash tests were conducted, and the compartment deformations of a small car in a crash into a medium car, MPV and SUV were compared. The structural interaction was poor in the SUV collision, and the passenger compartment of small car collapsed. Even structural interaction was good, a relatively large intrusion of the small car occurred in an MPV (multi-purpose vehicle) crash. Force matching and compartment strength will be significant for the next phase of compatibility improvement.

INTRODUCTION

Compatibility is defined as the ability to protect not only the occupants, but also other road users as well. Analyses of global accident data of car-to-car collisions from various countries have indicated that there are vehicles with low compatibility, such as cars with poor self-protection and cars with high aggressivity with respect to other cars. The aggressivity of SUVs has become an issue in the United States and to a lesser extent, Australia, as has the self-protection of small cars in Europe. In Japan as well, vehicle sizes vary widely, and compatibility is considered an important problem. It is therefore necessary to evaluate and improve compatibility performance based on crash tests.

Test procedures for evaluating and improving the compatibility of passenger cars are currently under discussion in the IHRA Compatibility Working Group [1]. Japan considers the activities of the IHRA to be a significant way to inform future legislation and regulation, and has conducted research with the aim of making an active contribution to these activities. The proposed IHRA phase 1 approach used a full-width test [1]. In the proposal, barrier force distributions are measured and evaluated to improve structural interaction. To have enough resistance force in the common interaction zone to avoid structural misalignment of SUV is considered as short term as phase 1a.

This paper summarizes the results of crash tests that Japan has conducted and reported to the IHRA Compatibility Working Group from 2003 to 2005. In the tests, the full-width rigid barrier (FWRB) test and full-width deformable barrier (FWDB) tests were compared with respect to barrier force distributions, vehicle deformations, vehicle accelerations, injury readings and SEAS detection. This study also includes the analysis of Australia PDB test to investigate the compartment strength. Car-to-car crash test series of small cars was examined, and the compartment intrusion was compared with respect to the structural interaction and compartment strength.

LOAD CELL WALL IN FULL-WIDTH TESTS

In full frontal tests, the barrier force distributions are measured from load cells, and structure alignment and homogeneity which are effective for structural interactions, are evaluated. Since Japan has a full-width rigid barrier crash test requirement in the regulation, it will be useful if the compatibility can be evaluated in this test configuration. In the present study, force distributions in full-width rigid and deformable barrier crash tests were examined from the data of JMLIT compatibility project and JNCAP (Japan New Car Assessment Program) tests.

Figure 1 shows the load cell alignment of IHRA agreement [1] and of JMLIT test series at a JARI test facility. The common interaction zone in IHRA is at row 3 and 4, which is from 330 mm to 580 mm above ground level. At JARI, the ground clearance of the load cell wall is 125 mm, and the area of rows 2, 3 and 4 correspond to rows 3 and 4 in the IHRA agreement load cell alignments.

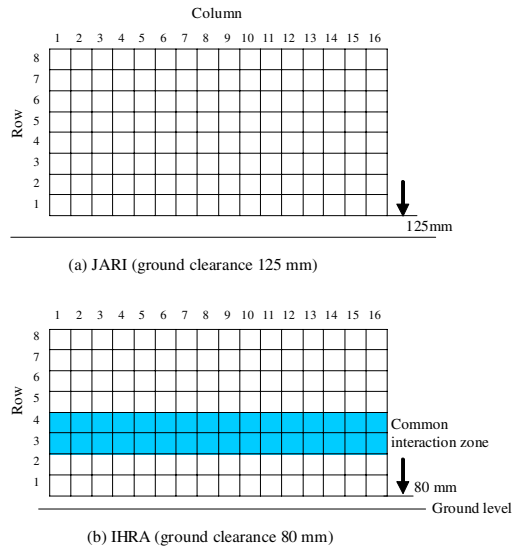

Figure 1. Alignment of load cell wall in JARI test facility and in IHRA agreement.

FULL-WIDTH DEFORMABLE BARRIER TESTS

Full-width deformable barrier tests were carried out for five vehicles using a deformable element developed by the Transport Research Laboratory (TRL) [1][2]. The first layer of the deformable element has a crush strength of 0.34 MPa with 150 mm depth, and the second layer has a crush strength of 1.71 MPa with 150 mm depth. Test vehicles include the minicar, small car, medium car, small SUV, MPV, and SUV that have different load paths (Table 1). Hybrid III dummies were used in driver and front passenger seats. An impact velocity was 55 km/h.

Table 1.
Test matrix of full-width deformable barrier tests.

Test car model	Vehicle class	Load path	Kerb mass (kg)	Test mass (kg)
Suzuki Wagon R	Minicar	Single (w/o bumper beam)	840	1041
Toyota Vitz (Yaris)	Small car	Single	921	1091
Subaru Legacy	Medium Car	Single (stiff lower Cross member)	1510	1699
Subaru Forester	Small SUV	2-stage (subframe)	1443	1638
Honda Stepwgn	MPV	Single (stiff lower Cross member)	1530	1717
Toyota Surf	SUV	Single (frame-type, SEAS)	1878	2076

Test vehicles after tests are presented in Figure 2. Generally, it was observed that the deformable element excites shear deformation of structures in the full-width deformable tests, which is similar in car-to-car crashes. The lower cross members and SEAS deformed rearward. Thus, the forces of the lower cross member which can prevent underride will be assessed effectively in the full-width deformable barrier tests.

As shown in Figure 2, the deformation of bumper rearward bending was observed in full-width deformable barrier tests, which is a different deformation mode in full-width rigid barrier crash tests. In a Legacy, according to the rearward bending of stiff bumper beam, the front-ends of longitudinal members bent and wrapped inside at the point where the cross-section area changes. Sensors attached to the front end of longitudinal members also may not work as designed when the longitudinal member deforms in this way. This inward deformation of longitudinal members was observed more or less for all tested vehicles, except the Wagon R, which does not have a bumper beam, and the thin longitudinal members penetrated the honeycomb.

Distributions of each load cell peak force are presented in Figure 3. The engine impact forces are mitigated by the deformable barrier, and forces of structures in a longitudinal direction can be seen clearly. Especially for Surf or Stepwgn, the longitudinal members are so stiff that they bottomed out the barrier, and the barrier force from these structures became high. The Forester has a subframe, Surf has a SEAS, and Stepwgn has a stiff lower cross member. If these lateral structures are stiff enough, they push the honeycomb and transfer forces at the barrier, though the force levels from lateral structures are not so high.

(a) Wagon R

(b) Vitz

(c) Legacy

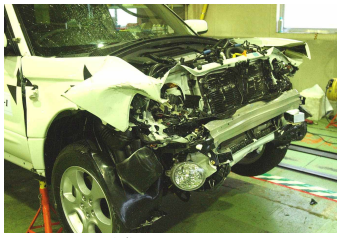

(d) Forester

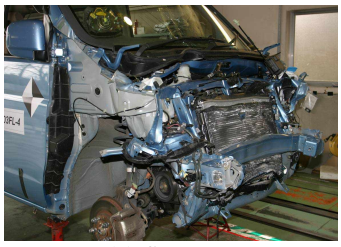

(e) Stepwgn

(f) Surf

Figure 2. Vehicle deformation in full-width deformable barrier tests.

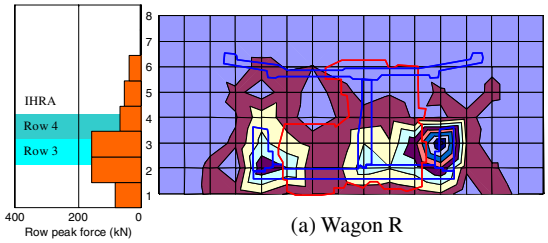

(a) Wagon R

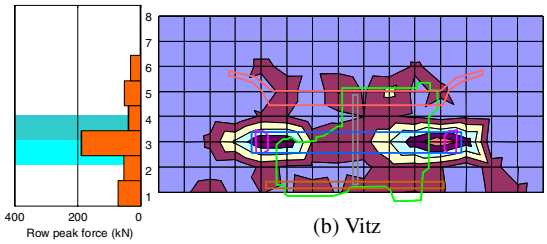

(b) Vitz

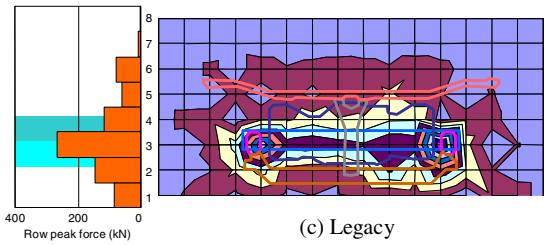

(c) Legacy

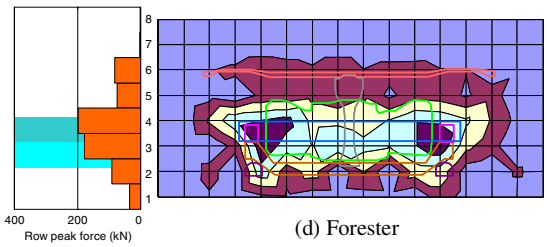

(d) Forester

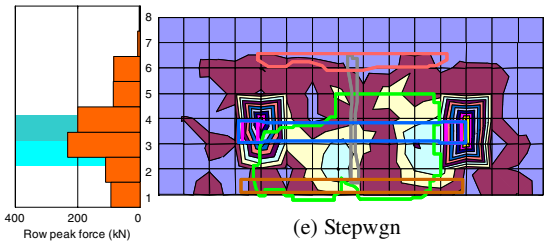

(e) Stepwgn

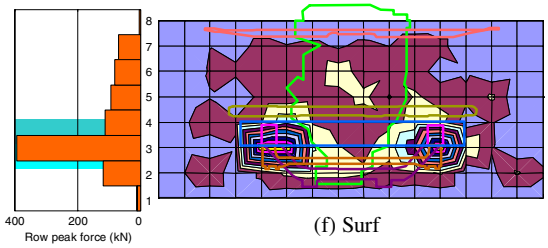

(f) Surf

Figure 3. Peak cell force in full-width deformable barrier tests.

The VNT is the difference of row force from a minimum target row load, which was proposed by TRL [1]. The VNT is a criterion to evaluate the reaction force in common interaction zone. The VNT is calculated as:

$$VNT = \sum_{Row(i)=3}^{4} IF\left[\{R_i \le TR\}THEN, ABS(R_i - TR), ELSE = 0\right]$$

where $R_i = \sum_{j=1}^{allcolumns} f_{ij}$,

f_{ij} = peak cell force.

The VNT will be an effective parameter to evaluate the resistance force in the common interaction zone if the target load level is selected properly. In the IHRA, the target row load is proposed as 100 kN. As shown in Figure 4, since the ground-height of the longitudinal member of Wagon R is low, the force level in row 4 became small. As the Vitz has a single load path, only force in row 4 is large. Though the VNT is a criterion of resistance force for SUV structural alignment, the row load of minicar and small car can be smaller than the target row load of 100 kN.

The HNT (horizontal component of negative deviation from target cell load) is also proposed by TRL as:

$$HNT = \sum_{Row(i)=3}^{4} \sum_{Column(j)=-2}^{+2} IF\left[\{f_{ij} \le TC_i\}THEN, ABS(f_{ij} - TC_i), ELSE = 0\right]$$

where TC_i is a target cell load calculated as:

$$TC_i = \frac{\sum_{j=1}^{allcolumns} f_{ij}}{(80\%\,\text{vehicle width})/(\text{load cell width})}.$$

The HNT is a parameter to evaluate the bumper beam stiffness. In Figure 4, the HNT of the tested vehicles is also shown. The HNT is good for Legacy and Forester which has a stiff bumper beam. The HNT is not good for other cars with a less-stiff bumper beam. The HNT is not also good for the SURF which has stiff longitudinal members. The HNT depends on the bumper beam stiffness as well as longitudinal member stiffness because TC_i heavily depends on the longitudinal member stiffness. Accordingly, it will be difficult to distinguish between the less-stiff bumper beam and the stiff longitudinal members on the basis of HNT. It might not be realistic to consider that an extremely stiff bumper beam is needed for vehicles with stiff longitudinal members. Further investigation will be needed for the HNT to evaluate the bumper beam stiffness.

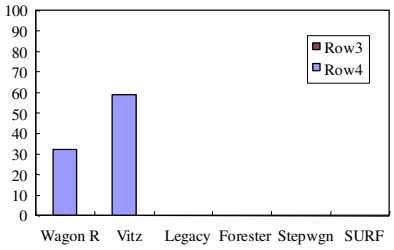

(a) VNT

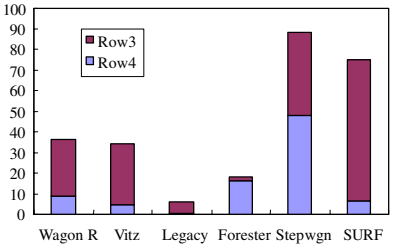

(b)HNT

Figure 4. VNT and HNT in full-width deformable barrier crash tests.

COMPARISON OF FULL-WIDTH RIGID AND DEFORMABLE BARRIER TESTS

Criteria of Structural Interaction

AHOF The AHOF in full-width deformable and rigid barrier tests were compared and shown in Figure 5. The AHOF measured in both barriers have a strong correlation. The honeycomb may affect the pitching of vehicles on impact, which can lead to higher AHOF. The AHOF of the Stepwgn and Wagon R in full-width deformable barrier tests are lower than in full rigid barrier tests, because the upper structures of these vehicles do not contact the whole barrier due to the limited size of the deformable element.

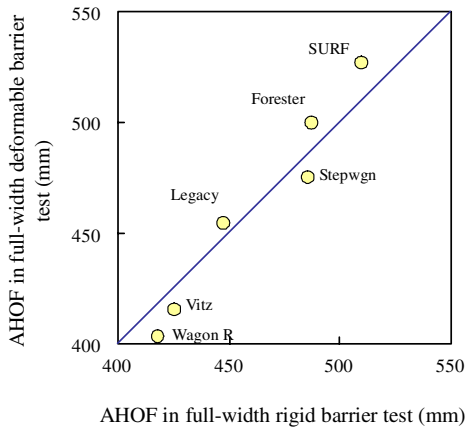

Figure 5. Average height of force in full-width rigid and deformable barrier tests.

Barrier Row Force Levels Estimated in Full Rigid Barrier Crash Tests In order to examine the target load level of 100 kN in full-width deformable barrier tests, the peak row load in the current vehicles was investigated using full-width rigid barrier test data. Figure 6 shows the sum of peak cell force in rows 3 and 4. As there is a correlation between the peak row load in full-width rigid and deformable barrier tests, the peak row loads in full-width rigid barrier tests were used for analysis. Figure 7 shows the sum of peak force in all load cells. The total peak cell forces in full-width rigid and deformable barrier tests have a linear relation, and the slope is 1.3. Therefore, the target row load of 100 kN in full-width deformable barrier tests will correspond to 130 kN in full-width rigid barrier tests.

Figure 8 shows the peak row force of minicars, small cars, medium and large cars, MPV and SUV in full-width rigid barrier crash tests. Due to low ground-height of longitudinal members, the peak force in rows 2 and 3 of some minicars is more than 130 kN whereas the peak force in row 4 is smaller than 130 kN. For many cars, the peak force in row 3 is higher than rows 2 and 4 because the longitudinal members contact row 3. This concentration of peak row force in row 3 will shift to rows 3 and 4 in the IHRA agreement load cell alignment since the longitudinal members will bridge between rows 3 and 4 in the IHRA alignment. However, some small cars and minicars will not satisfy the target row load of 100 kN in full-width deformable barrier tests.

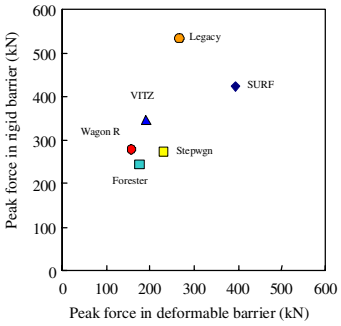

(a) Row 3 peak force

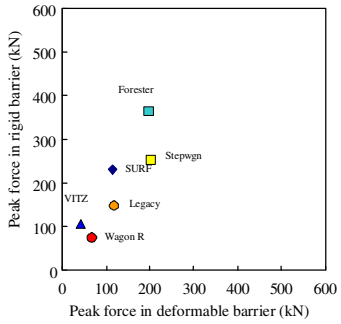

(b) Row 4 peak force

Figure 6. Peak row forces in rows 3 and 4 in full-width rigid and deformable barrier crash tests.

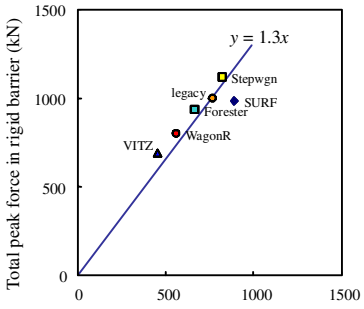

Figure 7. Total peak cell force in full-width rigid and deformable barrier crash tests.

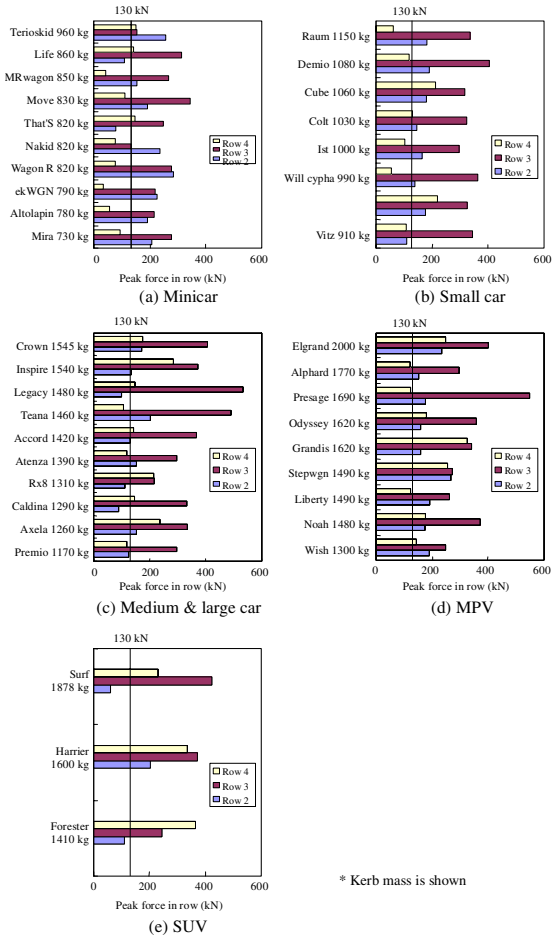

Figure 8. Peak cell force in row 2, 3 and 4 of vehicles in full-width rigid barrier crash tests.

Vehicle Acceleration and Dummy Responses

The dummy response and car acceleration of Wagon R are shown in Figure 9. The data also include the results of a car-to-car full frontal crash test with identical car models (Wagon R). The results of the full frontal car-to-car crash test are quite similar to those of full-width rigid barrier test. Because of a crash sensing time difference between rigid and deformable barrier tests, the dummy

restraint start times were later in deformable barrier tests compared with rigid barrier test. In the full-width deformable barrier test, the chest acceleration delayed and there is no peak around 25 ms by the seat belt pretensioner. As a result, the interaction of seat belt and airbag with dummies differed in both tests. The rear-loaded crash pulse in the full-width deformable barrier test could also lead to higher injury criteria. The deformable barrier can cause relatively high injury criteria for small cars with high-deceleration.

Figure 10 shows injury criteria of the driver dummy in full-width rigid and deformable barrier tests. Dummy criteria were similar for full-width rigid and deformable barrier tests. For Wagon R, the injury criteria were relatively higher in the full-width deformable barrier test.

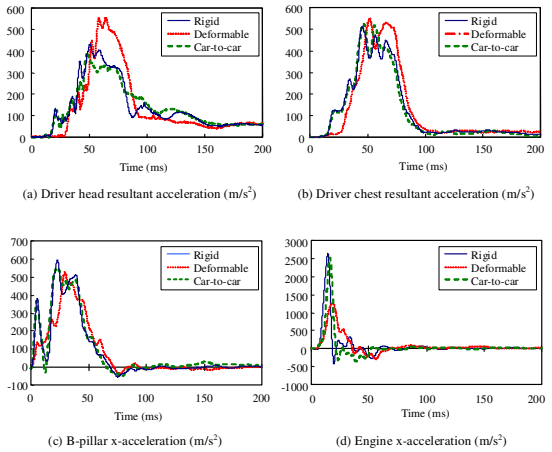

Figure 9. Dummy response and vehicle deceleration in full-width and deformble barrier tests.

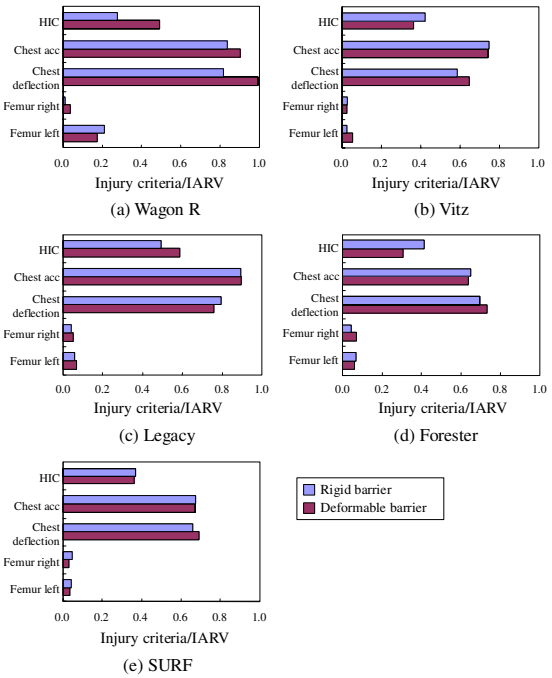

Figure 10. Dummy injury criteria in full-rigid and deformable barrier tests.

SEAS DETECTION IN FULL WIDTH DEFORMABLE BARRIER TESTS

Vehicle Deformation

In order to examine SEAS detection in force distributions in full-width tests, the force distributions of SUV with or without SEAS were examined. Test vehicles were an SUV (Toyota SURF) that has a frame-type longitudinal member with SEAS. The kerb mass of the vehicle is 1868 kg. Table 2 shows the test matrix. The results were compared to those of SURF with SEAS in full-width deformable and rigid barrier tests. The ground clearance of the load cell barrier was 125 mm. In this load cell alignment, the SEAS made contact with row 2 load cells. Thus, in this study, the VNT was calculated in rows 2, 3 and 4 though they are usually calculated in a common interaction zone (rows 3 and 4).

Figure 11 presents the SUV structure. The SEAS is mounted directly under the longitudinal member. From the front-edge of the bumper cover, the length of the bumper beam is 62 mm, and the SEAS is 377 mm in the longitudinal direction. In a case of SUV without SEAS, the SEAS were removed from the original SUV at the SEAS mount.

The vehicles after tests are shown in Figure 12. For the SUV with SEAS in the full-width deformable barrier test, the SEAS deformed rearward. In the full-width rigid barrier test, the SEAS did not deform rearward, and the SEAS made contact with the suspension cross member behind SEAS in accord with the collapse of longitudinal member. There were also differences in the deformation mode of longitudinal members. For the SUV with SEAS in the full-width deformable barrier test, the front-end of longitudinal members deformed downward in accord with to rearward bending of SEAS.

Figure 13 is a bottom view of the tested vehicle. For the SURF with SEAS, the deformation was symmetric between right- and left-hand longitudinal members. The front end of the longitudinal members deformed slightly inward (39.0 mm on the right-hand longitudinal member and 32.9 mm on the left-hand longitudinal member). On the other hand, for the SUV without SEAS, both longitudinal members deformed outward. The front end of the right-hand longitudinal member deformed 97.2 mm and the left-hand longitudinal member 15.1 mm because the longitudinal member became unstable due to removal of SEAS. As a result, they contacted a different location on the load cells from that of the original SUV with SEAS.

Table 2.
Test matrix of SUV in full-width tests to investigate SEAS detection.

Car model	Test	Impact velocity (km/h)	Test mass (kg)	Impact location from target
SURF with SEAS	FWDB	55	2076	20 mm (right side)
SURF without SEAS	FWDB	55	2076	7 mm (right side)
SURF with SEAS	FWRB	55	2076	18 mm (right side)

Figure 11. SEAS of SUV.

(a) with SEAS in FWDB test

(b) without SEAS in FWDB test

(c) with SEAS in FWRB test

Figure 12. Deformation of longitudinal member of SUV with and without SEAS in full-width deformable and rigid barrier test.

(a) with SEAS

(b) without SEAS

Figure 13. Bottom view of SUV with and without SEAS.

Peak Cell Force from SEAS

Peak cell force distributions of the SUV with and without SEAS are presented in Figures 14 and 15. There are smooth force distributions around the SEAS. In the row 2 where SEAS made contact, the row load was about 120 kN. On the other hand, in row 2 of SURF without SEAS, it was 87 kN. Thus, this test result supports the IHRA proposed threshold of 100 kN for target row load in the assessment area, which will be able to be achieved by attachment of the SEAS. The VNT of the SUV with SEAS is 0 kN for rows 2, 3 and 4. The VNT of the SUV without SEAS is 13, 0, 0 kN for rows 2, 3, and 4, respectively. Thus, the VNT can be a useful criterion to assess the reaction force of SEAS.

In the test of SURF with or without SEAS, lateral shifts from a target location were 20 mm and 7 mm in the test (see Table 2). As shown in Figure 15, the left-hand longitudinal member can also contact adjacent load cell with such a small shift in tests. For the SURF without SEAS, the longitudinal member became unstable with bending, and also contacted more than one load cells (rows 3, 4 and 5), which led to different force distribution around the longitudinal member.

Figure 16 presents the peak cell forces for the SUV with and without SEAS. Row 2 with columns from 6 to 12 are the load cells which are in alignment with the SEAS. From these two graphs, it may be still difficult to conclude that the forces of row 2 were generated from SEAS deformation. This is because there are many load cells with small forces in the force distribution where the vehicle makes contact.

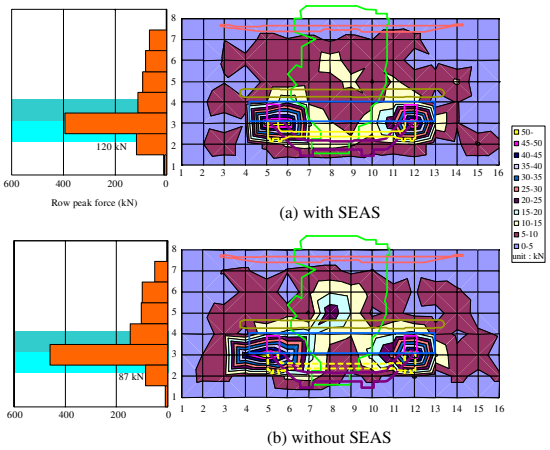

Figure 14. Peak cell force distributions of SUV with and without SEAS in full-width deformable barrier tests.

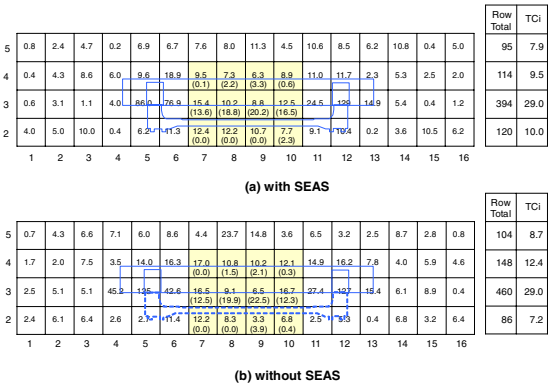

Figure 15. Peak cell force of SUV with and without SEAS to calculate VNT and HNT.

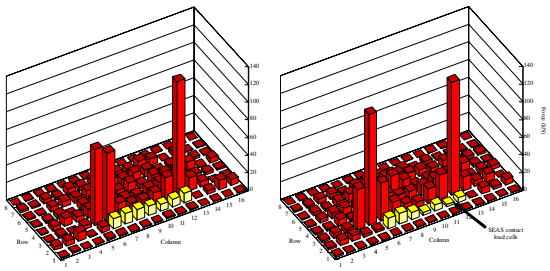

(a) with SEAS (b) without SEAS

Figure 16. Bar chart of peak cell force of SUV with and without SEAS in full-width deformable barrier tests.

The sum of the barrier force in row 2 where SEAS made contact was plotted against the vehicle displacement (Figure 17). The vehicle displacement was calculated from a double integral of the compartment acceleration. The force increases from the vehicle displacement of 0.4 m, where the SEAS began to contact the barrier. For the SUV without SEAS, the force level is small in the initial stage, and it increases after 0.5 m where lateral suspension structures start to contact the barrier. Consequently, it is considered that the barrier force in row 2 shows the SEAS reaction force in the full-width deformable barrier test. The result of SUV with SEAS in a full-with rigid barrier test is also shown in Figure 17. The force in row 2 does not increase until the deformation of 0.5 m. Since the vehicle deformation is flat in a rigid barrier test, the SEAS did not deform rearward and did not generate a reaction force against the barrier. Thus, it will be difficult to measure a SEAS reaction force in full-width rigid barrier crash tests.

The center of force (COF) was plotted with vehicle displacement (Figure 18). The COF is almost constant as the tested SUV which has a simple frame-type longitudinal member. The COF is smaller for the SUV with SEAS after the contact of SEAS. The average height of force (AHOF) was 527 mm for SUV with SEAS, and 552 mm without SEAS. There are several factors which can affect the AHOF such as engine impacts [3]. The criteria based on forces from row 2 such as VNT, may be a direct way to evaluate the SEAS reaction force compared to the AHOF.

The relative homogeneity assessment was calculated and shown in Figure 19. The homogeneity assessment was larger for the SUV with SEAS. Several factors can be considered for this reason. One is that the SUV longitudinal member was instable without SEAS, and contacted different load cells from the original SUV with SEAS. For SUV without SEAS, the impact forces of the engine became great due to bending of the left-hand longitudinal member, which also reduced the homogeneity assessment. Consequently, the load cell contact locations can significantly affect the barrier force distributions and homogeneity assessment. The influence of SEAS reaction force can be seen only for the homogeneity assessment in row which can be an override/underride criteria. Further investigation will be needed for the homogeneity assessment.

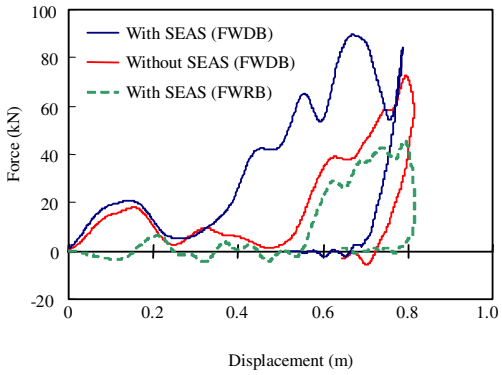

Figure 17. Barrier force in row 2 vs. vehicle displacement for SUV with and without SEAS in full-width deformable and rigid barrier tests.

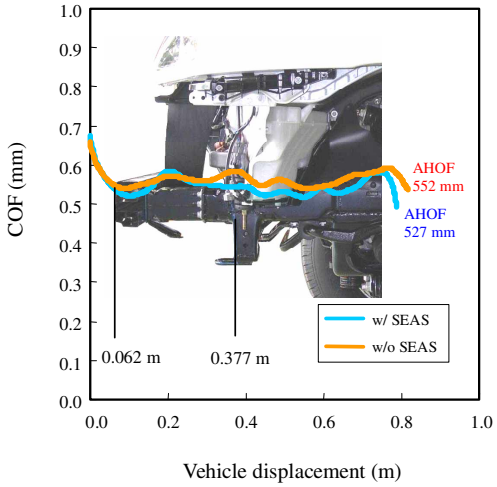

Figure 18. COF with vehicle displacement in full-width deformable barrier tests of SUV.

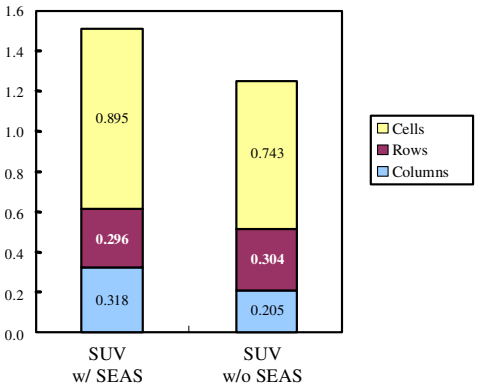

Figure 19. Relative homogeneity assessment in full-width deformable barrier tests of SUV.

EVALUATION OF COMPARTMENT STRENGTH IN PDB TESTS

Using Australian government data, the barrier forces in PDB tests were examined with respect to the compartment strength. The Australian government conducted PDB (progressive deformable barrier) offset tests using the Toyota Vitz (Echo or Yaris) at 60 and 74 km/h, and Vitz II at 74 km/h [4]. The Vitz has a simple structure with a single load path with two longitudinal members and a bumper beam. The Vitz II is a Vitz with a minor change, and the passenger compartment was strengthened from Vitz, whereas the front structures remain the same. The test data were provided by the Australian government.

The force-time histories of three tests are shown in Figure 20. In general, the barrier forces are similar in three tests although the Vitz passenger compartment collapsed in the 74 km/h test. The maximum force is the highest for the test at the lowest impact velocity of 60 km/h. The passenger compartment strength was evaluated based on criteria [5] (Figure 21). In the present study, the end of crash force is defined as the barrier force at the time when the engine acceleration is minimum after the engine makes contact with a firewall. However, it is rather difficult to determine the end of crash force in an objective way because the engine does not bottom out the barrier and engine acceleration is small during engine intrusion into the passenger compartment. The rebound force is a barrier force when the car separates from the barrier, and is determined from force-displacement curves. From the rebound force, the compartment strength is higher for the Vitz II than for the Vitz, which is a reasonable result. However, the rebound force is smaller for the Echo at 60 km/h than that at 74 km/h, even though the rebound forces are similar between 64 km/h and 80 km/h in tests using the EEVC barrier.

Because the PDB is deep and does not bottom out for cars, the barrier force may be difficult to use as criteria for compartment strength evaluation in an objective way. This situation is different from overload 80 km/h or ODB (offset deformable barrier) 64 km/h tests where the EEVC barrier bottoms out and the compartment resistance force can be transferred directly to the barrier force. According to PDB tests of the Vitz and Vitz II, the vehicle deformation mode is more similar to that in car-to-car crash tests compared to ODB tests. Thus, in PDB tests, the intrusion into the passenger compartment may be a reliable criterion for compartment strength evaluation.

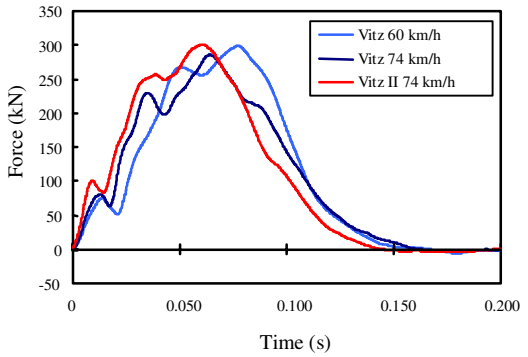

Figure 20. Barrier force-time histories in PDB tests.

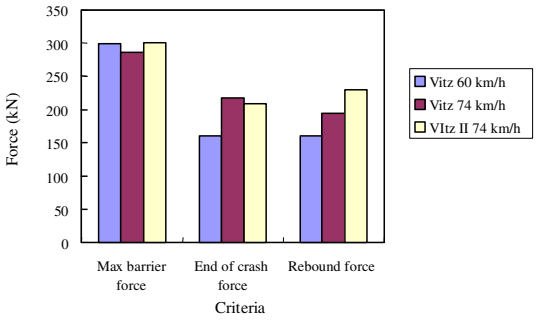

Figure 21. Passenger compartment strength criteria in PDB tests.

CAR-TO-CAR CRASHES

A series of car-to-car crash tests using a small car (Toyota Vitz) were conducted to investigate the structural interaction and compartment strength (Table 3). In the crash test series, the impact velocity was 50 km/h for both cars. The kerb mass of the Vitz is about 920 kg, and the test mass about 1090 kg. In Table 3, Vitz vs. Legacy crash test were conducted by the Australian government [4]. In order to examine the structural interaction, the SEAS was removed from the SURF.

Table 3.
Car-to-car crash test with Toyota Vitz. Impact velocity is 50 km/h.

Subject car	Other car			
	Model	Load path	Kerb mass (kg)	Test mass (kg)
Vitz	Legacy (Medium car)	1.5 Single (still lower cross member)	-	1600
Vitz II	Legacy (Medium car)	1.5 Single (still lower cross member)	1430	1589
Vitz II	Surf (SUV) w/o SEAS	Single Frame-type, SEAS was removed)	1906	2076
Vitz II	Odyssey (MPV)	2-stage (subframe)	1660	1830

Figures 22 and 23 show the deformation of Vitz. The crash test between the Vitz, Vitz II and Legacy demonstrated the effectiveness of passenger compartment strength. By stiffening the passenger compartment from Vitz to Vitz II, the A-pillar rearward displacement was reduced from 118 mm to 33 mm. The longitudinal member of Vitz made contact above the bumper beam of Legacy and deformed in upward direction. Therefore, the structural interaction was not still so good.

In a crash into a SURF which the SEAS was removed, the longitudinal member of SURF did not interact with the Vitz II longitudinal member, and it made contact the suspension strut, which induced a large intrusion into the passenger compartment of the Vitz II. The A-pillar rearward displacement of the Vitz was 349 mm. The right femur force of the driver dummy was more than the injury threshold (13.4 kN). If the SEAS was not removed from the original SURF, the SEAS could interact with a right-hand tire of the Vitz, and poor structural interaction would be improved.

In a crash into an Odyssey, the structural interaction was good, and the front structure of the Vitz absorbed the energy efficiently. However, due to the force mismatch between vehicles, the steering axis of the Vitz moved upward (100 mm), which led to high chest acceleration of the driver dummy (56.5G).

The crash test results demonstrate that after good structural interaction, there will not be a significant compartment collapse. However, there may be no end to control passenger compartment intrusion until the guidelines for force-matching and compartment strength are provided.

Vitz (vs. Legacy)

Vitz II (vs. Legacy)

Vitz II (vs. SURF w/o SEAS)

Vitz II (vs. Odyssey)

Figure 22. Passenger compartment deformation in car-to-car crashes.

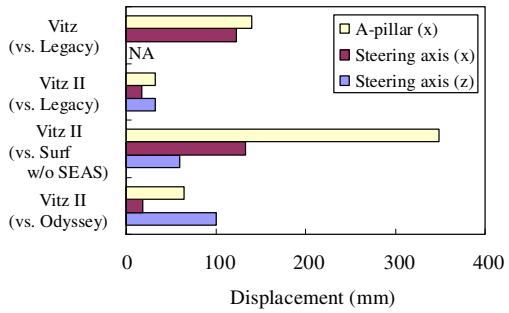

Figure 23. Passenger compartment intrusion of small car in car-to-car crashes.

DISCUSSION

In the present research, full-width rigid and deformable barrier crash tests were compared using a series of crash tests. A deformable element in full-width tests will be useful because shear deformation of the structures occurs and the local force of engine impact is mitigated. However, in full-width deformable barrier crash tests, for some cars with stiff bumper beam, the longitudinal members deformed in an unnatural mode in accord with rearward bending of the bumper beam. This deformation mode can affect sensor timing, especially with a seat belt pretensioner. Particularly for minicars and small cars, the deformable barrier effect is large because of the high acceleration of these cars, and the sensor delay can affect occupant interaction with airbag. It is still not clear how minicars or small cars optimized in full-width deformable barrier tests can affect the crashworthiness of these cars in real-world collisions.

Barrier forces of SUV with or without SEAS were examined. The results indicate that a reaction force from the SEAS can be evaluated using the peak row load in full-width deformable barrier crash tests. The target row load of 100 kN will be an acceptable threshold because the peak row load at the SEAS location decreased from 120 kN to 87 kN by removal of SEAS. Although it is also important for minicars and small cars to have longitudinal members with a ground-height in alignment with common interaction zone, further research will be needed to apply the SUV target row load 100 kN to minicars and small cars. This is because after ODB 64 km/h tests in NCAP, the compartment accelerations of minicars and small cars are already so high that high reaction forces required in common interaction zone can induce higher car acceleration, and acceleration-related injuries to occupants can increase even at low speed impacts.

The car-to-car crash test series using small cars indicated that the lateral and vertical mismatch of the longitudinal member can lead to the passenger compartment collapse of the small car. This situation will be improved after IHRA phase 1, when the structural interaction of SUV becomes acceptable. Although minimum strength of the passenger compartment is significant means to prevent the passenger compartment collapse, too strong a passenger compartment, on the other hand, can induce acceleration-related injuries. After structural interaction is improved, the stiffness matching and compartment strength will be important in controlling the intrusion and deceleration of the passenger compartment. The force matching and the compartment strength are important especially for the vehicle fleet where passenger cars occupy a large population like Japan.

CONCLUSIONS

A series of crash tests was carried out to assess vehicle compatibility. The results are summarized as follows:

1. Shear deformation occurs in full-width deformable barrier crash tests, and lateral members generate forces on the load cell barrier though the force level is small.
2. Full-width deformable barrier crash tests can be used as high acceleration tests. However, in full-width deformable barrier crash tests, the longitudinal member deformed inward, which can induce a crash sensor delay.
3. SEAS was detected in a full-width deformable barrier test, and VNT with a target row load of 100 kN will be a useful criterion to evaluate its force level.
4. Car-to-car crash tests showed that the guidelines of force matching and compartment strength will be needed to control and predict the passenger compartment intrusion.

ACKNOWLEGEMENTS

The authors thank the Australian Government, Department of Transport and Regional Services for providing crash test data.

REFERENCES

[1] O'Reilly, P., "Status Report of IHRA Compatibility and Frontal Impact Working Group," 19th ESV, 2005.

[2] Edwards, M., Davies, H., Hobbs, A., "Development of Test Procedures and Performance Criteria to Improve Compatibility in Car Frontal Collisions," 18th ESV, Paper Number 86, 2003.

[3] Mizuno, K., Tateishi, K., Arai, Y., Nishimoto, T., "Research on Vehicle Compatibility in Japan," 18th ESV, Paper Number 113, 2003.

[4] Seyer K., Newland C., Terrell, M., "Australian Research to Develop a Vehicle Compatibility Test," International Journal of Crashworthiness, Vol.8, No.2, pp.143-150, 2003.

[5] Mizuno, K., Arai, Y., Newland C.A., "Compartment Strength and its Evaluation in Car Crashes," International Journal of Crashworthiness, Vol.9, No.5, pp.547-557, 2004.